Transactions, SMiRT-23
Manchester, United Kingdom - August 10-14, 2015
Division VII, Paper ID 373

A CASE STUDY OF SCENARIO EARTHQUAKE-BASED RISK ASSESSMENT FOR NUCLEAR POWER PLANTS

Mohamed M. Talaat[1], David K. Nakaki[2], Philip S. Hashimoto[3], Gregory S. Hardy[3], Robert P. Kennedy[4], and Robert P. Kassawara[5]

[1] Senior Staff Engineer, Simpson Gumpertz & Heger Inc, USA; Adjunct Assistant Professor, Cairo University, Egypt
[2] Senior Project Manager, Simpson Gumpertz & Heger Inc, USA
[3] Senior Principal, Simpson Gumpertz & Heger Inc, USA
[4] RPK Structural Mechanics Consulting, Escondido, CA, USA
[5] Principal Technical Leader, Electric Power Research Institute, USA

ABSTRACT

This paper presents an application of a proposed scenario earthquake-based approach for nuclear power plant (NPP) seismic probabilistic risk assessment (SPRA) and compares it to traditional SPRA. Traditional time history response analysis for SPRA of NPPs uses a relatively limited number of acceleration time histories which are matched to a site-specific uniform hazard spectrum (UHS). The response and capacity probability distributions are combined to construct seismic fragilities of the NPP structures, systems, and components (SSCs). The plant logic model is used to combine the SSC fragilities into a plant-level fragility, which is convolved with seismic hazard to compute seismic core damage frequency. The scenario earthquake approach uses a large number of recorded time histories with unmodified spectral shapes. The scenario time histories are assigned individual occurrence rates and scale factors, such that the aggregate statistics of their spectra reproduce the site hazard.

This case study quantifies the seismic risk calculated using the two approaches for a representative NPP structure and site hazard. The NPP structure is modeled using a lumped-mass stick model. We calculated the UHS-based fragility using a suite of thirty spectrum-matched time histories, and compared the resulting mean annual frequency of failure (MAFF) to scenario-based MAFF from 602 scenarios. We explicitly modeled the effects of structure property uncertainty using Latin Hypercube Sampling (LHS) with sixty realizations and verified the effect of the LHS procedure on the stability of the results. The scenario-based MAFF of the structure was calculated to be about 60% of the UHS-based MAFF. The results showed comparable stability in the risk estimate with respect to the randomization procedure.

This paper presents the methodology and case study results for the NPP structure. Extension of these results to SPRA studies requires developing similar comparisons for component failure probabilities inside the structure, and depends on the relative importance of SSCs in the plant logic model.

INTRODUCTION

Traditionally computed structure response in SPRA studies may introduce conservatism because the UHS does not represent realistic strong motion spectral shapes. Rather, it combines ground motions from nearby and distant sources. Consequently, UHS-matched earthquake records excite multiple structure modes simultaneously with ground motions that have the same individual (i.e. not joint) probabilities of being exceeded. This approach assumes perfect correlation between spectral ordinates. Baker (2011) showed that this correlation is a function of the frequency shift between the two modes and proposed the Conditional Mean Spectrum (CMS) alternative to the UHS. Abrahamson and Al-Atik (2010) proposed a method for developing realistic earthquake scenario records for conducting seismic response analysis.

The scenario records are chosen from a database of original records initially screened against some selection criteria (e.g., magnitude and distance ranges that control the hazard at the site). The spectral shapes of the scenario records are preserved. The scenario records are assigned scale factors and occurrence rates iteratively selected until the aggregate statistics of the resulting spectra exhibit a good match to the site hazard (Abrahamson and Yunatci, 2010). Each unique record in the database can be used to create several scenarios by assigning multiple scale factors and corresponding occurrence rates. This enables the creation of a large suite of scenarios (on the order of a thousand) from a limited number of unique records (on the order of a hundred). The Electric Power Research Institute has conducted a multi-year study into the use of scenario earthquake to conduct more accurate SPRA for NPPs.

HAZARD AND GROUND MOTIONS

Site Hazard

The ground motion hazard was characterized by the geometric mean of the horizontal component peak ground acceleration (PGA) and a reference UHS shape. The spectral shape is representative of a Western United States (WUS) site and corresponds to 1E-04 Mean Annual Frequency of Exceedance (MAFE). Only the horizontal direction records were used in this case study. The PGA mean hazard curve is plotted in Figure 1a. The reference UHS is shown in Figure 1b. The reference PGA value is 0.421g.

UHS Earthquake Acceleration Records

The ground motion set consisted of thirty records of two components each. The geometric mean of the horizontal components was spectrally matched to the mean UHS curve (Figure 2a). To account for horizontal component-to-component directional variability, a set of thirty equal-probability multipliers were randomly generated using the LHS method, from a lognormal distribution with a median of 1.0 and a standard deviation of 0.18. One component of each record pair was multiplied by the directional variability multiplier and the orthogonal record was divided by it, thus maintaining the geometric mean values. Figure 2b shows these multipliers overlaid on the distribution.

Scenario Earthquake Acceleration Records

The ground motion set consisted of 602 pairs of horizontal scenario records. These scenario records were scaled from seventy-four unique database records, with distance and magnitude ranges of 1 km to 25 km and 5.5 to 7.6, respectively. Each scenario was assigned an annual rate of occurrence, so the scenario set recreated the UHS at ten discrete levels defined between 1E-02 and 1E-07 MAFE. The assigned scenario rates of occurrence ranged from 3.6E-11/year to 4.5E-04/year. The aggregate rate of occurrence of these scenarios was 0.0111/year. Since the unique database records represented recorded ground motions (filtered and baseline corrected), the two horizontal components were scaled together to preserve the distribution of directional variability. The aggregate scenario spectra were calculated using Eqns 1 and 2.

$$MAFE(S_a) = \sum_{j=1}^{602} \nu_j \left[IF\left\{ S_{a,j} \geq S_a \right\} \right] \quad (1)$$

$$S_{a,j} = F_{k \to j} S_{a,k} \quad (2)$$

where S_a is the spectral acceleration value that is varied to calculate the hazard, ν_j is the occurrence rate per scenario, j is the scenario index, k is the index of the unique uncalled record in the database, and $F_{k \to j}$ is its scale factor for Scenario j. The aggregate statistics of the scaled scenario spectra are shown compared to the site UHS in Figure 3. The figure shows a good match in the MAFE range of 1E-03 to 1E-06, which typically controls the seismic risk.

CASE STUDY NPP STRUCTURE

The NPP structure model geometry is shown in Figure 4 and represents a typical reinforced concrete structure. This stick model consists of eight lumped masses at floors above the foundation. The structure model seismic response was simulated using computer program CLASSI (Luco and Wong, 1980). CLASSI performs linear-elastic finite element (FE) response history analysis of the structure model in the frequency domain. Soil-structure interaction (SSI) can be modelled in CLASSI for foundations idealized as rigid. In this case study, the foundation was modelled as fixed-base to avoid additional complexity.

Median Model of NPP Structure

The median masses and stiffnesses of the model were selected to produce a fundamental horizontal frequency of 8.0 Hz, which is representative of NPP structures. The first three natural vibration modes and mode shapes in the horizontal direction are summarized in Table 1 and Figure 4. About 76% of the structure mass participates in the first mode. The first three modes combined account for about 99% of the structure mass, and are well-separate at frequencies of 35 HZ or lower. A median structure damping ratio of 7% was assigned independent of frequency.

Modelling of Variability in Structure Response

Sixty randomized computer models of the structure were generated to account for uncertainty in the dynamic properties. The modal frequencies of the structure were represented using a lognormal distribution with a median value of 1.0 and a standard deviation of 0.15. The damping ratios were represented using a lognormal distribution with a median of 1.0 and a standard deviation of 0.35. Sixty equal-probability sets of frequency and damping ratio variability multipliers were randomly generated using the LHS method from the aforementioned distributions and multiplied by the median values to create the sixty randomized computer models. Figure 5b shows these multipliers overlaid on their respective distributions.

In the UHS-based response analysis, the sixty randomized structure models were randomly assigned to the thirty sets of ground motion records (i.e., each ground motion record set was assigned to two structure models). The sixty pairs of ground motion record sets and structure models were input to computer program CLASSI (Luco and Wong, 1980) to conduct the probabilistic response history analysis. Using this stratified sampling approach, the total number of response-history analysis runs was sixty.

In the scenario-based response analysis, the stratified sampling approach described above could not be made to generate statistically stable results. The scenario records represent earthquakes of significantly disparate strengths, frequencies of occurrence, and risk contribution. Therefore, the random assignment of structure model realizations to the scenario records made the risk results sensitive to the subset of structure model realizations assigned to the subset of scenario records that contribute the most to the risk. Typically, these are less than thirty records out of 602, with about five records accounting for 25% of the risk or more. The scenario records were therefore each assigned to the sixty structure model realizations and run independently, which resulted in a distribution of sixty possible responses per scenario. Using this approach, the total number of response-history analysis runs was $60 \times 74 = 4{,}440$. Since linear response-history analysis was performed, the seismic responses to the 602 scenarios were scaled from the seismic responses to the seventy-four unique records that produced them.

Modelling of Structure Capacity Distribution

The structure capacity was expressed in terms of seismic base shear. A median base shear capacity was assigned in each direction. This median base shear capacity was based on the seismic base shear demand

from three deterministic response-history analyses, which was considered to represent design-level demand. The three deterministic analyses used one of the thirty spectrally-matched ground motion records and three structure models with best-estimate, upper-bound, and lower-bound frequencies. The latter two models used frequencies of 1.162 and 0.861 times the median frequencies, which correspond to a lognormal standard deviation of 0.15. The envelope of the design-level base shear demand was multiplied by a design safety factor of 2.5 to define the median capacity. Based on later review of the probabilistic response distribution, the structure failure was found to be controlled by base shear capacity, Q, in the X-direction, which has a median value of 663,000 MN. A lognormal standard deviation β_Q = 0.20 was assigned for uncertainty in the base shear capacity.

PROBABILISTIC SEISMIC RESPONSE DISTRIBUTIONS

UHS-Based Base Shear Distribution and Seismic Fragility

The X-direction seismic base shear demand, V, has the 60-count histogram shown in Figure 6a at the reference PGA value of 0.421g. A lognormal fit to the data is shown with a median of 258,000 MN and a lognormal standard deviation β_V = 0.16. The fitted distribution shows a good match, with slight conservatism in the lower 80% of the distribution and slight non-conservatism between 80% and 95% percentiles. The corresponding mean conditional probability of structure failure at the reference earthquake level can be calculated by convolution of the response and capacity distributions. Since both random variables are lognormally distributed, this probability can be simply calculated by constructing a new random variable, F_s, equal to the ratio of the capacity to the demand. The new random variable represents the scale factor on the reference earthquake that would make the demand equal to the capacity. It has the median and lognormal standard deviations given by Eqns 3 and 4, respectively. The conditional probability of failure at the reference earthquake is given in Eqn 5.

$$\check{F}_s = \check{Q}/\check{V} = 663{,}000/258{,}000 = 2.57 \tag{3}$$

$$\beta_C = \sqrt{\beta_Q^2 + \beta_V^2} = 0.26 \tag{4}$$

$$P_{FAILURE|REF.EQ} = P(Q \le V|REF.EQ) = P(F_s \le 1|REF.EQ) = \Phi\left(\frac{ln(1)-ln(\check{F}_s)}{\beta_C}\right) = 0.00014 \tag{5}$$

where β_C is the composite lognormal standard deviation and represents variability for both randomness and uncertainty, and Φ is the cumulative standard normal distribution function. In the UHS-based SPRA methodology, the seismic fragility is traditionally expressed as the conditional probability of failure given the reference ground motion parameter (Kennedy and Reed, 1994). The mean seismic fragility is defined as a lognormal distribution with the median PGA capacity, A_m, defined in Eqn 6, and composite lognormal standard deviation β_C = 0.30 (Eqn 4).

$$A_m = \check{F}_s PGA_{REF} = 2.57 \times 0.421g = 1.08g \tag{6}$$

Scenario-Based Base Shear Distribution

The X-direction base shear responses for each scenario earthquake record constitute a distribution of sixty data points. Figure 6b shows the X-direction base shear distribution for Scenario 451, which was found to have the biggest contribution to seismic risk, discussed later in this paper. A lognormal fit to the data from an individual scenario shows a poor fit and is inadequate. Figure 7 shows a summary of all 60 × 602 scenario responses. Unlike the UHS-based responses, each scenario base shear distribution (e.g. Figure 6b) represents responses to disparate ground motions and rates of occurrence. To summarize these

distributions, they were combined as follows: The 36,120 base shear responses were ordered largest to smallest; each response was assigned the mean annual rate of occurrence for the corresponding scenario; and for each response value a MAFE was then calculated as the sum of mean annual rates of occurrence from the present response value up to the highest response. Figure 7 also plots the MAFEs of the conditional failure probabilities associated with the base shear realizations, where the relationship between the two plots on the main and secondary axes is explained by the arrows on the figure.

STRUCTURE SEISMIC RISK QUANTIFICATION

UHS-Based MAFF

The mean annual frequency of failure for the structure was calculated by convolution of the mean seismic fragility (Figure 6b) and seismic hazard (Figure 1a) curve. The convolution was performed numerically by discretizing the seismic hazard into eight bins, as defined in Table 2. The risk contribution of each bin is the product of the corresponding occurrence frequency and the conditional failure probability at the representative PGA obtained from the structure seismic fragility. The structure UHS-based MAFF was summed from all eight hazard bins to be 1.83E-06. Figure 8a shows the percentage risk contributions of the different hazard bins. As typically observed in SPRA studies, the risk is controlled by the moderate earthquakes, with PGA in the range of 0.7g to 1.1g contributing about two-thirds of the risk.

Scenario-Based MAFF

The scenario-based risk was calculated as the sum over the 602 scenarios of the product of scenario occurrence rate and average conditional failure probability per scenario, according to Eqn 7. The average conditional failure probability per scenario was defined as the average of the sixty individual probabilities of failure (i.e. one for each simulated response, according to Eqn 8). The individual conditional failure probabilities were calculated according to Eqn 9.

$$MAFF = \sum_{j=1}^{602} \nu_j \bar{P}_{FAILURE|SCENARIO,j} \tag{7}$$

$$\bar{P}_{FAILURE|SCENARIO,j} = \frac{1}{60} \sum_{i=1}^{60} P_{FAILURE|SCENARIO,j}^{(i)} \tag{8}$$

$$P_{FAILURE|SCENARIO,j}^{(i)} = \Phi\left(\frac{ln\left(V_{SCENARIO,j}^{(i)}\right) - ln(\check{Q})}{\beta_Q}\right) \tag{9}$$

The structure scenario-based MAFF was summed from all 602 scenarios to be 1.07E-06. Figure 8b shows the percentage risk contributions of the different scenarios. The figure shows that only seven out of the 602 scenarios contribute more than 3% of the seismic risk each. These risk-significant scenarios have occurrence rates between 1E-07 and 1E-06. About one-third of the total risk is due to these seven scenarios combined. Furthermore, about one-half of the total risk is due to the top-scoring fifteen scenarios, while the remaining 587 scenarios account for the other half.

Comparison of UHS-Based and Scenario-Based Risk Approaches

The scenario-based seismic risk of the case study structure is about 60% of the traditional UHS-based value. This reduction in risk is attributed to the reasons summarized in the introduction, particularly the conservatism inherent in using UHS-matched motions to develop response distributions for a structure with well-separated dynamic modes. The significance of this reduction in structure seismic risk estimate on SPRA studies cannot be directly assessed without further investigation. It should be combined with the corresponding effect of the scenario-based approach on seismic risk estimates of systems and

components housed in the structure, and on the relationships between the different SSCs within the plant logic model. Equipment dynamic responses and seismic capacities may be controlled by a single frequency each, rather than multiple modes. This case study further investigated the scenario-based seismic risk of hypothetical equipment components dominated by single-frequency responses and housed in the NPP structure, which is the subject of a future paper. The equipment components were assigned a range of typical median frequencies of 5, 8, and 12 Hz (i.e., below, at, and above the structure fundamental frequency) and corresponding spectral acceleration capacity distributions. The scenario-based component seismic risk estimates did not consistently increase or decrease relative to the UHS-based values, and as a general trend they increased. The overall impact of adopting this scenario-based SPRA methodology is not yet conclusive and depends on the relative risk significance of each SSC. A simple logic model consisting of all the SSCs connected in series had an increased scenario-based risk.

The sensitivity of the risk numbers to the LHS randomization procedure was assessed using an alternate randomization. A different set of randomized structure properties was generated by re-combining the pairs of stiffness and damping multipliers randomly to generate sixty new structure model realizations. The probabilistic time-history analyses were performed one more time. The response distribution was processed to compute a seismic fragility and a set of conditional scenario failure probabilities from the alternate randomization. The alternate UHS- and scenario-based MAFF values were 2.11E-06 and 1.13E-06, respectively. The alternate randomization resulted in differences of about 15% and 5% in the UHS-based and scenario-based MAFF results, respectively. These discrepancies are small compared to the typical uncertainties present in SPRA results. The risk results are therefore stable with respect to the randomization procedure. The stability of the scenario-based results is comparable to UHS-based studies.

The difference in effort required to conduct probabilistic scenario-based seismic response analysis is not trivial compared to the UHS-based counterpart. The stratified LHS approach typically employed for the latter was proved inadequate for earthquake scenarios. The number of response analysis runs employed in this study therefore increased from 60 to 4,440; i.e., the total number of UHS-based simulations equals the number of simulations required for only one unique scenario record. For a typical number of unique records on the order of a hundred, this is a hundred-fold increase in simulation time. This study did not consider SSI effects, which are typically required for many NPP structures. Since the scenario records represent a range of events with disparate magnitudes and occurrence rates, there is nontrivial additional effort involved in developing strain-compatible soil profiles consistent with each group of scenarios.

CONCLUSION

We performed a case-study application of scenario-based SPRA for a representative fixed-base NPP structure and site hazard, and compared it to traditional UHS-based SPRA. The UHS-based analysis employed thirty acceleration records spectrally matched to the mean 1E-04 UHS horizontal geomean with directional variability added. The earthquake scenarios employed 602 scaled records whose aggregate spectra reproduced the site hazard. Uncertainty in the structure response was modelled using the LHS method with sixty stratified structure model realizations. A base shear capacity probability distribution was assigned to the structure. The response distributions were obtained from both analyses and compared to the capacity distribution to compute conditional probabilities of failure, which were then convolved with the hazard data to compute the structure MAFF. The scenario-based structure seismic risk was 60% reduced from the UHS-based risk, and had comparable stability with respect to the LHS randomization procedure. This reduction was observed in the structure seismic risk estimate alone. Its effect on the overall plant risk depends on the corresponding changes in system and component seismic risk estimates and on the plant logic model. These dependencies are explored in a future paper. The additional effort and complexity involved in performing a scenario-based SPRA study is significant, and should be considered against the expected improvement in risk assessment accuracy, taking into account the types of dominant risk contributors for the plant.

REFERENCES

Abrahamson, N.A., and Al-Atik, L. (2010). "Scenario Spectra for Design Ground Motions and Risk Calculation." 9th US/10th Canadian Conference on Earthquake Engineering, Toronto, Canada.

Abrahamson, N.A., and Yunatci, A.A. (2010). "Ground Motion Occurrence Rates for Scenario Spectra." Fifth International Conference on Recent Advances in Geotechnical Earthquake Engineering and Soil Dynamics, San Diego, California, USA.

Baker, J.W. (2011). "Conditional Mean Spectrum: Tool for Ground Motion Selection." *Journal of Structural Engineering,* 137(3), 322-331.

Kennedy, R.P. and Reed, J.W. (1994). *Methodology for Developing Seismic Fragilities*, EPRI TR-103959, Electric Power Research Institute, Palo Alto, California, USA.

Luco, J.E. and H.L. Wong (1980), *Soil-Structure Interaction: A Linear Continuum Mechanics Approach (CLASSI)*, Report No. CE79-03, University of Southern California, Los Angeles, California, USA.

Table 1 – Structure Model Horizontal Modes and Fractions of Total Mass Participation

Mode	Frequency	Fraction of Total Mass Participation		
	Hz	X	Y	Z
1	8.00	0.764	0.000	0.000
2	22.83	0.171	0.000	0.000
4	34.77	0.052	0.000	0.000

Table 2 – Seismic Hazard Bins for Risk Quantification

Hazard Bin	Range	Representative PGA (g)	Frequency (/yr)
1	0.09g ≤ PGA < 0.3	0.16	4.14e-03
2	0.3g ≤ PGA < 0.5g	0.39	3.22e-04
3	0.5g ≤ PGA < 0.7g	0.59	3.42e-05
4	0.7g ≤ PGA < 0.9g	0.79	5.78e-06
5	0.9g ≤ PGA < 1.1g	0.99	1.30e-06
6	1.1g ≤ PGA < 1.3g	1.20	3.26e-07
7	1.3g ≤ PGA < 1.5g	1.40	5.06e-08
8	PGA >1.5g	1.65	1.00e-07

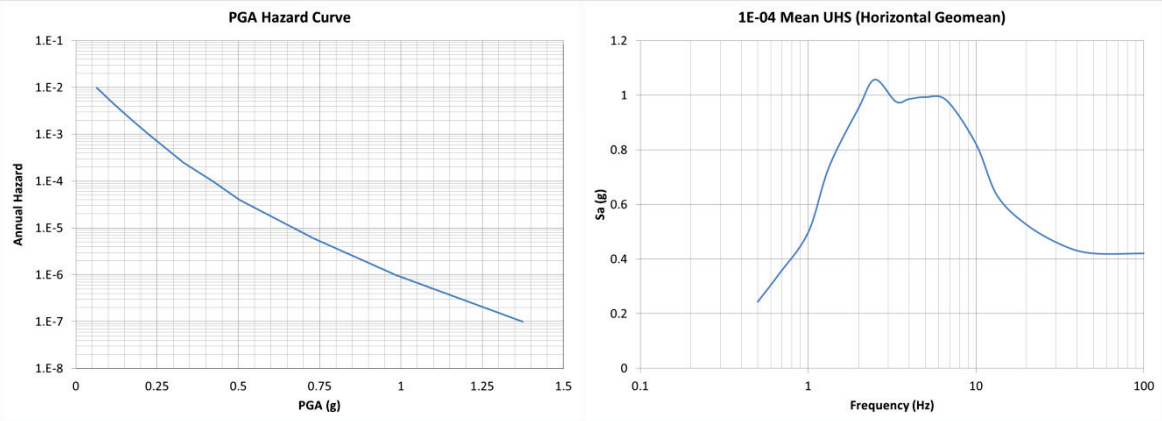

(a) PGA Hazard Curve (b) Mean Uniform Hazard Spectrum

Figure 1 – Site Hazard

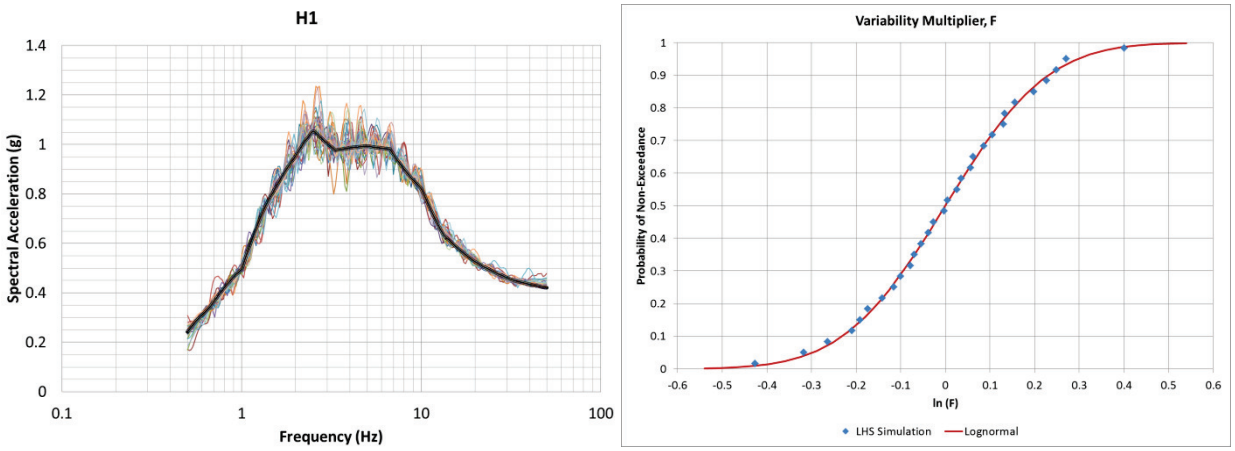

(a) Comparison of H1 Direction to Geomean (b) Directional Component Variability Multipliers

Figure 2 – Spectral Match of UHS-Based Records

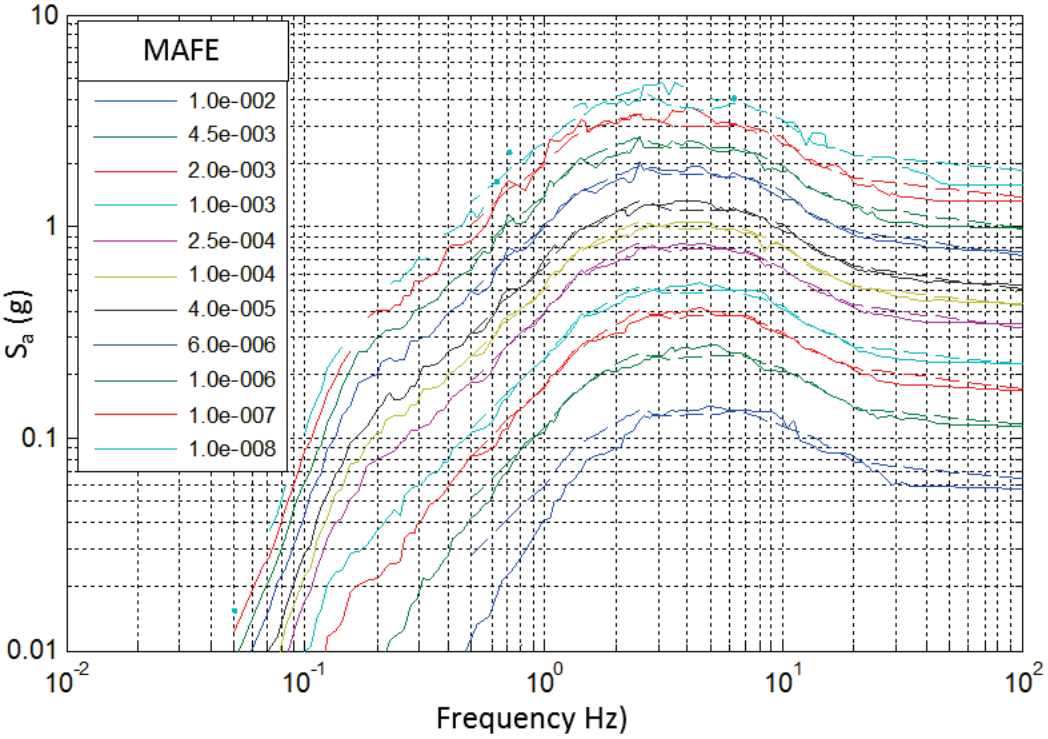

Figure 3 – Reproduction of UHS Spectra from Scenario Records

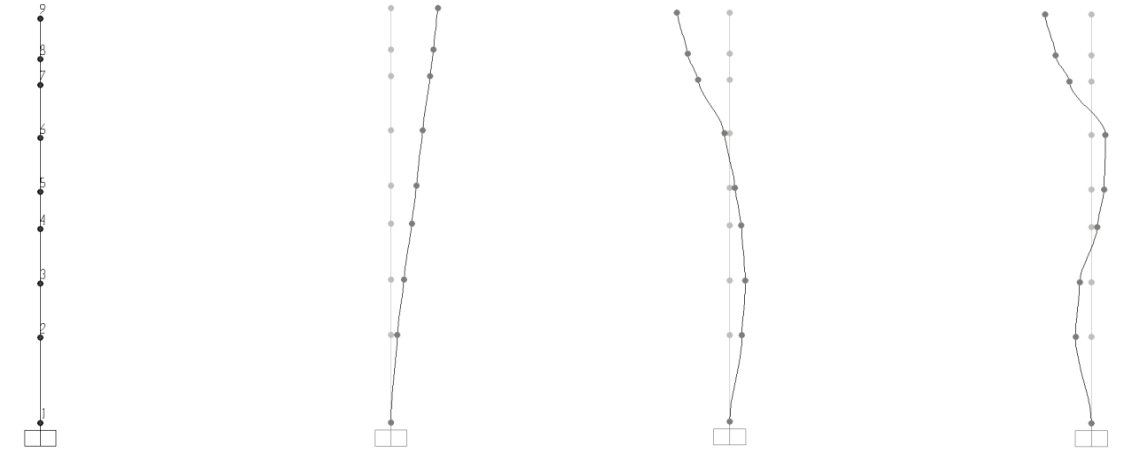

Figure 4 – Median Case Study Structure Model

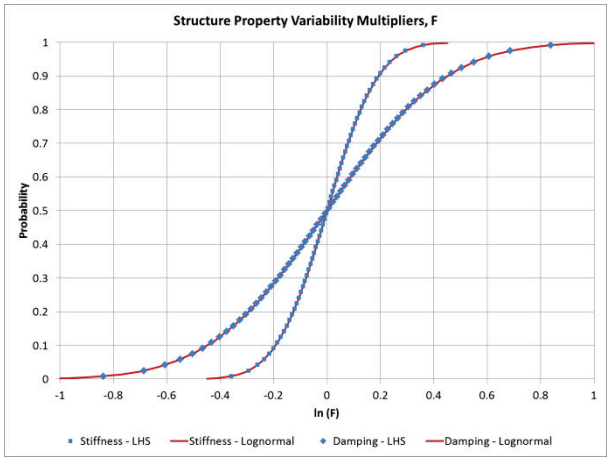

Figure 5 – Structure Model Property Variability Multipliers

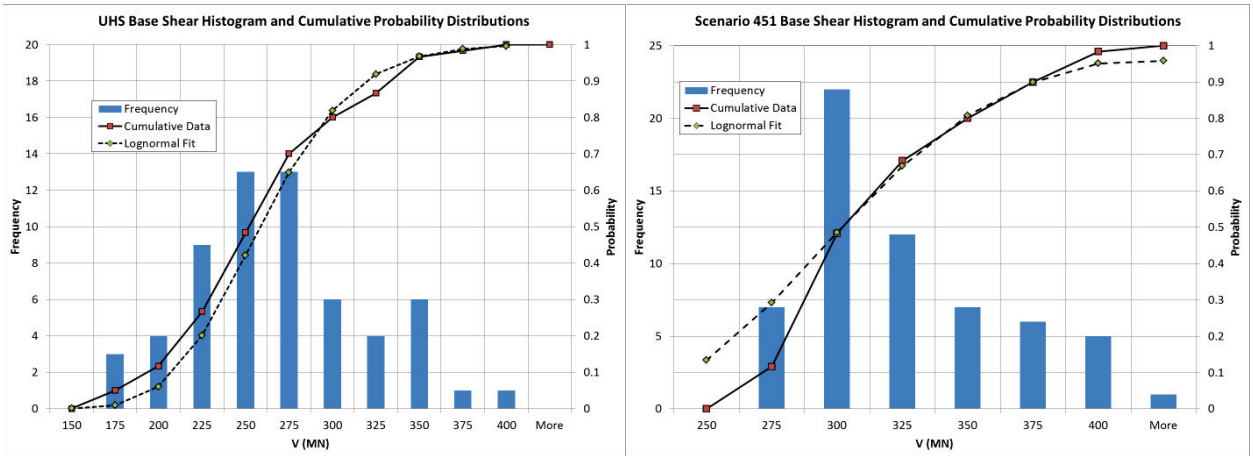

(a) Responses to UHS-Matched Records (b) Responses to Highest-Risk Scenario

Figure 6 – X-Direction Seismic Base Shear Response Distributions

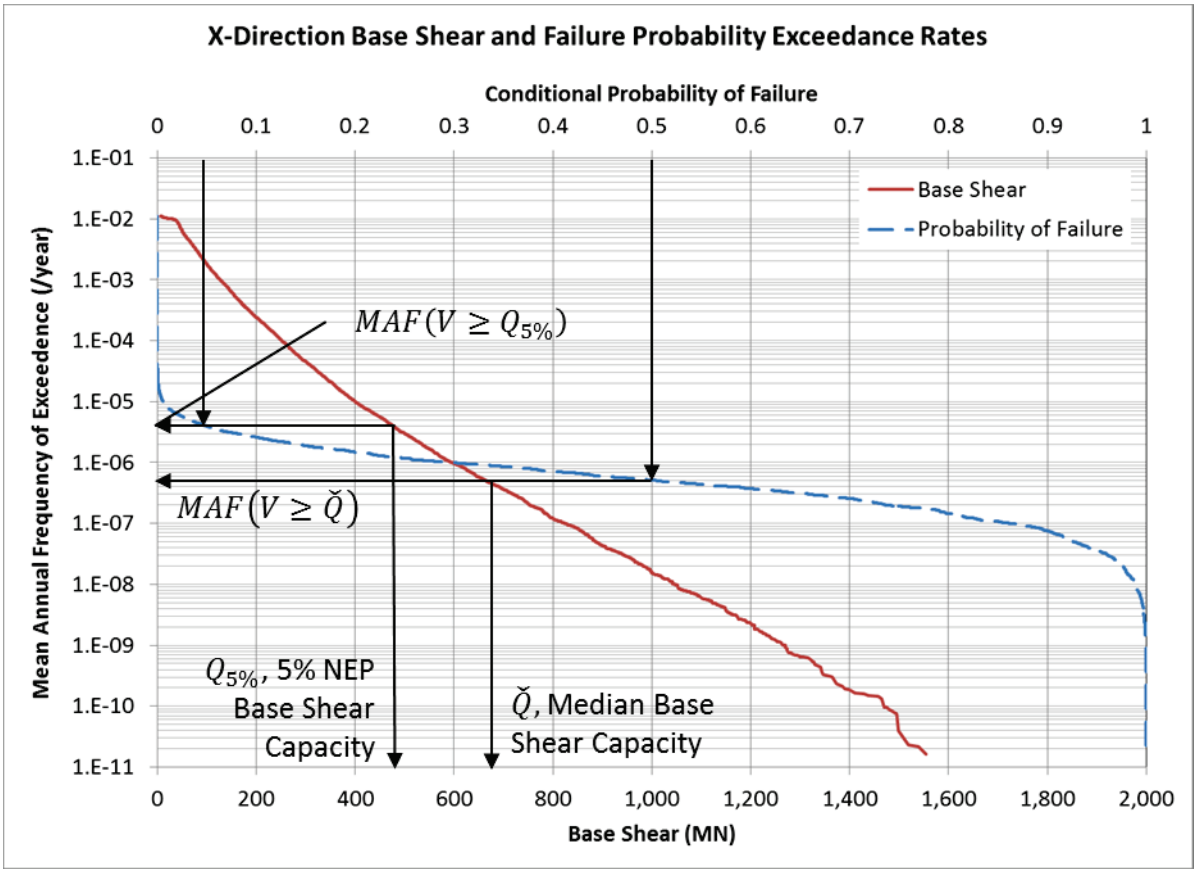

Figure 7 – Scenario-Based Base Shear Mean Annual Frequencies of Exceedance

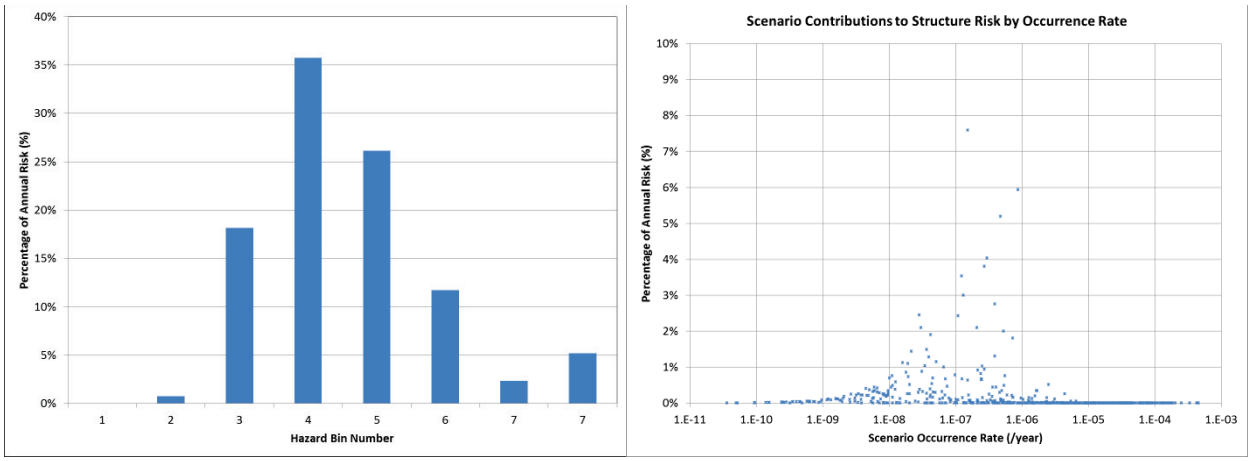

(a) from UHS-Based Hazard Bins (b) from Individual Scenario Records

Figure 8 – Percentage Contributions of Initiating Events to Structure Seismic Risk